Full-profile refinement by derivative difference minimization

Leonid A. Solovyov

Full-profile refinement by derivative difference minimization

Leonid A. Solovyov

Institute of Chemistry and Chemical Technology, 660049 Krasnoyarsk, Russia. Correspondence
e-mail: leosol@icct.ru

A new method of full-profile refinement is developed on the basis of the minimization of the derivatives of the profile difference curve. The use of the derivatives instead of the absolute difference between the observed and calculated profile intensities allows refinement independently of the background. The procedure is tested on various powder diffraction data sets and is shown to be fully functional. Besides having the capability of powder diffraction structure analysis without modelling the background curve, the method is shown to allow the derivation of structure parameters of even higher quality than those obtained by Rietveld refinement in the presence of systematic errors in the model background function. The derivative difference minimization principles may be used in many different areas of powder diffraction and beyond.

1. Introduction

The Rietveld (1969) method is widely applied as a standard technique of structure refinement from powder diffraction data (Young, 1993; McCusker *et al.*, 1999). Its evident advantage is the possibility of using experimental data in the initial form of a full powder diffraction profile. This process, in turn, requires the modelling of all of the scattering contributions to a powder pattern, including the background. In simple cases, the background can be estimated and subtracted from a powder profile (Sonneveld & Visser, 1975; von der Linden *et al.*, 1999; Fischer *et al.*, 2000; David & Sivia, 2001) or modelled by physically based functions (Riello *et al.*, 1995). However, as a rule, the background line is very difficult to describe correctly, since it is a complex sum of different components originating from the sample itself, amorphous and semi-crystalline admixtures, the sample holder and other sources. Therefore, in most cases, the background in Rietveld refinement is accounted for by applying empirical functions such as polynomial or Fourier series. Of course, none of these empirical functions can provide an adequate general description of the background line. The only assumption that the empirical modelling is based on is the background line being a smooth curve slowly changing with diffraction angle. Thus the refinement may be aimed not at minimizing the absolute difference between the experimental and calculated profiles but at minimizing the oscillations (or curvature) of the difference curve. In this paper, a new approach to full-profile refinement is presented, based on the minimization of a reformulated aim function; this method does not require background line modelling. The approach is tested on both calculated and experimental data.

2. Derivative difference method

As a measure of the difference curve oscillations, the absolute values of its derivatives may be used. The corresponding minimization function can be chosen as

$$\sum \left\{ w^1 \left[\frac{\partial}{\partial \theta} (I_o - I_c) \right]^2 + w^2 \left[\frac{\partial^2}{\partial \theta^2} (I_o - I_c) \right]^2 + \cdots + w^k \left[\frac{\partial^k}{\partial \theta^k} (I_o - I_c) \right]^2 \right\}, \quad (1)$$

where I_o and I_c are the experimental and calculated profile intensities, θ is the diffraction angle, w is the weight and the sum is over the entire powder profile. Applying the Savitzky–Golay (SG) formalism (Savitzky & Golay, 1964) for the derivative calculation, we can write the minimization function as

$$\text{MF} = \sum_{i=m+1}^{N-m} \sum_k w_i^k \left(\sum_{j=-m}^{m} c_j^k \Delta_{i+j} \right)^2, \quad (2)$$

where c_j^k are the SG coefficients for the derivative of order k with the profile convolution interval $[-m, m]$, N is the number of points in the profile and Δ is the profile difference ($\Delta = I_o - I_c$). The variable structure and profile parameters, v_r, are refined by solving the normal equations corresponding to the minimum of (2),

$$\sum_k \sum_{i=m+1}^{N-m} w_i^k \left(\sum_{j=-m}^{m} c_j^k \Delta_{i+j} \right) \left(\sum_{j=-m}^{m} c_j^k \frac{\partial I_{c,i+j}}{\partial v_r} \right) = 0, \quad (3)$$

$$w_i^k = \left[\sum_{j=-m}^{m} (c_j^k)^2 (\sigma_{i+j})^2 \right]^{-1}, \qquad (4)$$

where σ_i is the variance in the experimental profile intensity I_{oi}. The sum in (4) represents the squared variance in the SG derivative of order k for the ith profile point. The standard deviations of the refined parameters can be estimated from the equation

$$s_i = [A_{ii}^{-1} \mathrm{MF}/(N - P + C)]^{1/2}, \qquad (5)$$

where A_{ii}^{-1} is the diagonal element in the inverted normal matrix, N is the number of observations, P is the number of refined parameters and C is the total number of constraints.

For a practical application, the set of k derivatives needs to be restricted to a finite number. Test runs of the procedure showed that the use of the first and second derivatives calculated applying the SG coefficients for the second-degree polynomial gave satisfactory results. When minimizing only the first-order derivative, the refinement was less stable since, presumably, the first derivative has values close to zero in the regions of the diffraction peak maxima, thus reducing the contribution of these regions to the minimization function. The SG coefficients for the first and second derivatives with the convolution interval $[-m, m]$ can be expressed as

$$c_j^1 = \frac{3j}{m(m+1)(2m+1)},$$

$$c_j^2 = \frac{45j^2}{m(m+1)(2m+1)[4m(m+1)-3]} - \frac{15}{(2m+1)[4m(m+1)-3]} \qquad (6)$$

The results of the derivative difference minimization (DDM) are dependent on the choice of the convolution intervals for each profile data point. On the one hand, the intervals should be narrow enough to provide an adequate calculation of the derivatives. On the other hand, the intervals should be wide enough to 'feel' the long oscillations of the difference curve. A derivative of the profile difference can, alternatively, be considered as a difference in the derivatives of the observed and the calculated profiles. Since the SG coefficients are calculated from a polynomial fitted to the profile convolution interval, the optimal convolution interval should be the maximal one that provides an adequate polynomial fitting of the observed profile. For simplicity, the intervals can be chosen to be equal to the average FWHM of the diffraction peaks. Preliminary tests of the procedure showed that such a choice provided stable refinement. However, better results were achieved by applying flexible convolution intervals for each profile point. The optimal intervals can be assigned on the basis of the counting statistics. The assignment procedure consists in finding the widest interval for which the average deviation of the observed profile intensities from the SG polynomial does not exceed one standard deviation of the intensity at each point of the convolution interval. This procedure generates narrow

convolution intervals for the powder profile regions with intense well resolved diffraction peaks, and wide intervals for the regions with small and/or overlapped peaks.

The reliability factor for DDM may be calculated analogously to the conventional Rietveld refinement as a normalized sum of the squared derivative difference over the powder profile. However, the value of such a reliability factor will be dependent on the convolution interval choice. For instance, for wider convolution intervals the R factor will be lower, because the wider the intervals the smoother the derivative curve. A more unbiased R factor can be calculated as

$$R_{\mathrm{DDM}} = \left[\frac{\sum_k \sum_{i=m+1}^{N-m} w_i^k \left(\sum_{j=-m}^{m} c_j^k \Delta_{i+j} \right)^2}{\sum_k \sum_{i=m+1}^{N-m} w_i^k \left(\sum_{j=-m}^{m} c_j^k I_{o,i+j} \right)^2} \right.$$

$$\left. + \frac{\sum_{i=m+1}^{N-m} w_i \left(I_{oi} - \sum_{j=-m}^{m} c_j^0 I_{o,i+j} \right)^2}{\sum_{i=m+1}^{N-m} w_i I_{oi}^2} \right]^{1/2}. \qquad (7)$$

The second summand in (7) characterizes the quality of the SG smoothing of the observed profile. This term will increase with increasing convolution interval, since with wider convolution intervals the quality of the SG polynomial fit is worse. Such a composite R factor allows a partial compensation of the R_{DDM} dependence on the convolution interval choice.

3. Results and discussion

The DDM algorithm can be easily adjusted to any Rietveld refinement program. It was included in a modified and corrected version of *BDWS*-9006*PC* (Wiles & Young, 1981) and tested on various data sets.

The first tests were performed using a calculated powder X-ray diffraction profile of $Ag_2[Pd(NH_3)_2(SO_3)_2]$ (Solovyov *et al.*, 1999). Numerous DDM runs starting from randomly altered structure and profile parameters showed stable and correct refinement, equivalent by the convergence rate to the least-squares Rietveld refinement. The initial structure model used for generating the test calculated profile was reproduced by DDM completely up to the isotropic displacement parameters. Comparative Rietveld and DDM refinements were performed on a calculated powder X-ray diffraction profile with simulated statistical noise and a polynomial background of moderate curvature. The resultant structural parameters are presented in Table 1. As seen, both Rietveld and DDM procedures allowed reproduction of the test structure at a similar accuracy, the highest bias being 0.007 Å for the $S-O3$ distance.

For a severe test, the calculated profile with simulated noise was added by a randomly oscillating highly curved background. DDM was again started from randomly altered parameters (with 0.5–1.0 Å displacement of the atomic posi-

tions) and demonstrated a stable convergence. The results are illustrated in Fig. 1. The test structure model was reproduced with less than 0.01 Å deviation in the interatomic distances.

Table 1
Fractional atomic coordinates, isotropic displacement parameters ($\mathrm{\AA}^2$) and selected interatomic distances (Å) after Rietveld and DDM refinements of a calculated powder X-ray diffraction profile of the $Ag_2[Pd(NH_3)_2(SO_3)_2]$ test structure.

	x	y	z	B_{iso}	Distances	
Test structure model						
Pd	0	0	0	0.26	Pd—N	2.078
Ag	0.43962	−0.23405	0.14784	1.36	Pd—S	2.288
N	−0.09560	0.15653	0.14846	0.50	S—O1	1.446
S	0.25150	0.26264	0.03578	0.24	S—O2	1.497
O1	0.44339	0.17397	0.11612	0.27	S—O3	1.478
O2	0.21362	0.46382	0.11336	0.27	Ag—O1	2.411
O3	0.25389	0.35499	−0.09626	0.27	Ag—Pd	3.296
Rietveld refinement						
Pd	0	0	0	0.29 (5)	Pd—N	2.080 (6)
Ag	0.4397 (1)	−0.2340 (2)	0.14787 (7)	1.33 (4)	Pd—S	2.290 (3)
N	−0.0959 (8)	0.1567 (8)	0.1485 (5)	0.5 (2)	S—O1	1.449 (5)
S	0.2518 (3)	0.2630 (5)	0.0359 (2)	0.19 (8)	S—O2	1.498 (6)
O1	0.4442 (8)	0.173 (1)	0.1156 (5)	0.4 (1)	S—O3	1.481 (7)
O2	0.2139 (7)	0.464 (1)	0.1139 (5)	0.4 (1)	Ag—O1	2.406 (6)
O3	0.2532 (8)	0.354 (9)	−0.0968(6)	0.4 (1)	Ag—Pd	3.297 (1)
DDM refinement						
Pd	0	0	0	0.30 (7)	Pd—N	2.079 (6)
Ag	0.4395 (1)	−0.2342 (2)	0.14782 (7)	1.34 (6)	Pd—S	2.289 (3)
N	−0.0985 (8)	0.157 (1)	0.1471 (5)	0.7 (2)	S—O1	1.450 (5)
S	0.2512 (3)	0.2632 (5)	0.0353 (2)	0.17 (8)	S—O2	1.501 (6)
O1	0.4433 (7)	0.1721 (8)	0.1151 (5)	0.2 (1)	S—O3	1.485 (7)
O2	0.2132 (6)	0.464 (1)	0.1139 (5)	0.2 (1)	Ag—O1	2.403 (5)
O3	0.2525 (7)	0.3555 (8)	−0.0978 (6)	0.2 (1)	Ag—Pd	3.296 (1)

Table 2
Experimental details.

Crystal data		
Chemical formula	$[Pd(NH_3)_4](C_2O_4)$	$(C_5H_6N)Al_3F_{10}$
Crystal system	Triclinic	Monoclinic
Space group	$P\bar{1}$	$C2/m$
a (Å)	7.1218 (1)	8.2699 (3)
b (Å)	7.0812 (1)	6.2014 (2)
c (Å)	3.8030 (2)	10.508 (1)
α (°)	91.913 (7)	90
β (°)	98.651 (7)	103.40 (1)
γ (°)	97.288 (5)	90
V (Å³)	187.80 (3)	524.22 (75)
Z	1	2
Radiation type	Cu $K\alpha$	Neutron
Wavelength (Å)	1.5418	1.8857
Temperature (K)	293	293
Data collection		
Data collection method	θ−2θ scan	θ−2θ scan
Increment in 2θ (°)	0.02	0.05
2θ range (°)	11–90	5–150
Refinement		
Refinement on	I_{net}	I_{net}
R_{wp}	0.055	–
R_{exp}	0.021	–
R_B	0.025	–
R_{DDM}	0.068	0.115
H-atom treatment	H atoms constrained	H atoms refined
Weighting scheme	Based on measured s.u. values	Based on measured s.u. values

The only notable bias from the test model was found in lower (by ∼0.5–0.7 $\mathrm{\AA}^2$) isotropic displacement parameters, B_{iso}. The randomly curved background line was reproduced by the difference curve in detail.

Further tests of the method were performed using experimental data. The DDM procedure was applied to the $[Pd(NH_3)_4](C_2O_4)$ structure (Solovyov *et al.*, 1996) in parallel with the conventional least-squares Rietveld refinement using the same powder X-ray diffraction pattern. The results are summarized in Tables 2–4 and the structure is shown in Fig. 2. The final agreement between the observed and calculated powder profiles obtained by applying the two methods is demonstrated in Fig. 3. Both the DDM and the Rietveld procedure gave satisfactory structure parameters. Moreover, the DDM refinement allowed the derivation of even better structural geometric characteristics. A smaller imbalance in the C—O distances and O—C—C angles of the oxalate molecule was obtained by DDM, and the C—C distance was much closer to that (1.54 Å) usually determined for oxalates. The problem with the Rietveld refinement in this case was, in particular, due to a local maximum of the background curve between 25 and 35° 2θ, which was not adequately modelled by the polynomial background function applied. Since DDM is
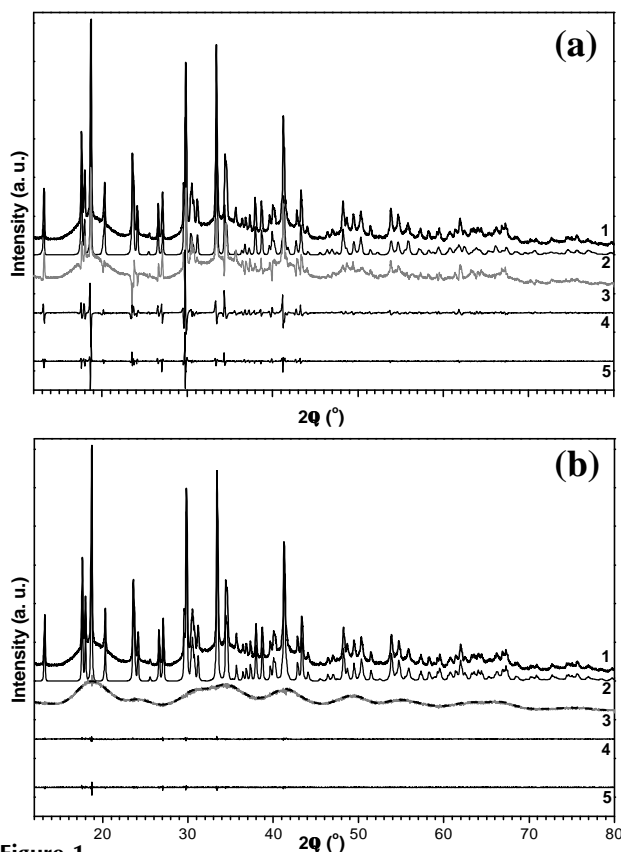

Figure 1
The results of the DDM refinement run on a test powder diffraction profile with a randomly curved background line added. The test (1), calculated (2), difference (3), difference first derivative (4) and difference second derivative (5) profiles are shown at the initial stage (*a*) and after 15 cycles of DDM (*b*). The dark dashed line in (*b*) represents the curved background line added.

Table 3
Fractional atomic coordinates and isotropic displacement parameters (Å^2) for $[Pd(NH_3)_4](C_2O_4)$.

	x	y	z	B_{iso}
DDM refinement				
Pd	0	0	0	1.11 (3)
O1	0.4339 (6)	0.2535 (6)	0.538 (1)	1.8 (1)
O2	0.7256 (6)	0.4173 (6)	0.533 (1)	1.8 (1)
C	0.545 (1)	0.405 (1)	0.519 (2)	1.6 (2)
N1	0.2659 (7)	−0.0660 (7)	−0.058 (2)	1.8 (1)
N2	0.0786 (7)	0.2796 (7)	−0.101 (1)	1.7 (2)
Rietveld refinement				
Pd	0	0	0	0.91 (3)
O1	0.4380 (5)	0.2569 (5)	0.538 (1)	1.1 (1)
O2	0.7274 (5)	0.4181 (4)	0.530 (1)	1.3 (1)
C	0.5533 (9)	0.4040 (8)	0.527 (2)	1.3 (2)
N1	0.2685 (5)	−0.0651 (5)	−0.058 (1)	1.3 (1)
N2	0.0826 (5)	0.2815 (5)	−0.100 (1)	1.0 (1)

Table 4
Selected geometric parameters (Å, °) for $[Pd(NH_3)_4](C_2O_4)$.

DDM refinement			
Pd—N1	2.049 (5)	N1—Pd—N2	91.2 (2)
Pd—N2	2.053 (5)	N1—Pd—N2^{ii}	88.8 (2)
C—C^i	1.564 (11)	O1—C—O2	125.5 (6)
C—O1	1.261 (8)	O1—C—C^i	117.7 (6)
C—O2	1.271 (8)	O2—C—C^i	116.8 (6)
Rietveld refinement			
Pd—N1	2.064 (4)	N1—Pd—N2	90.3 (1)
Pd—N2	2.070 (4)	N1—Pd—N2^{ii}	89.7 (1)
C—C^i	1.643 (9)	O1—C—O2	128.4 (6)
C—O1	1.248 (7)	O1—C—C^i	112.6 (5)
C—O2	1.230 (7)	O2—C—C^i	118.8 (5)

Symmetry codes: (i) $1 − x, 1 − y, 1 − z$; (ii) $−x, −y, −z$.

independent of the background, it allowed structure parameters of better quality to be obtained.

The DDM refinement was also tested on neutron diffraction data of $(C_5H_6N)Al_3F_{10}$ (Fig. 4), whose structure solution was performed in the framework of the 'DuPont Powder Challenge' (Harlow *et al.*, 1999). The problem with this structure
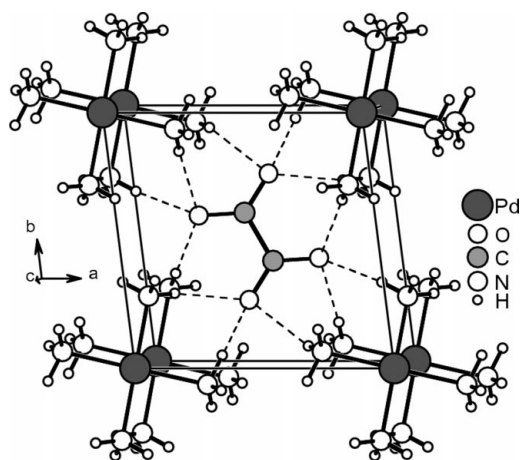
analysis was in the low quality of the powder diffraction data (Fig. 5) as a result of strong anisotropic peak broadening and complex background curvature. In the process of structure determination, the background was approximated by an enhanced variant of the algorithm described by Sonneveld & Visser (1975). The Rietveld refinement of the structure was
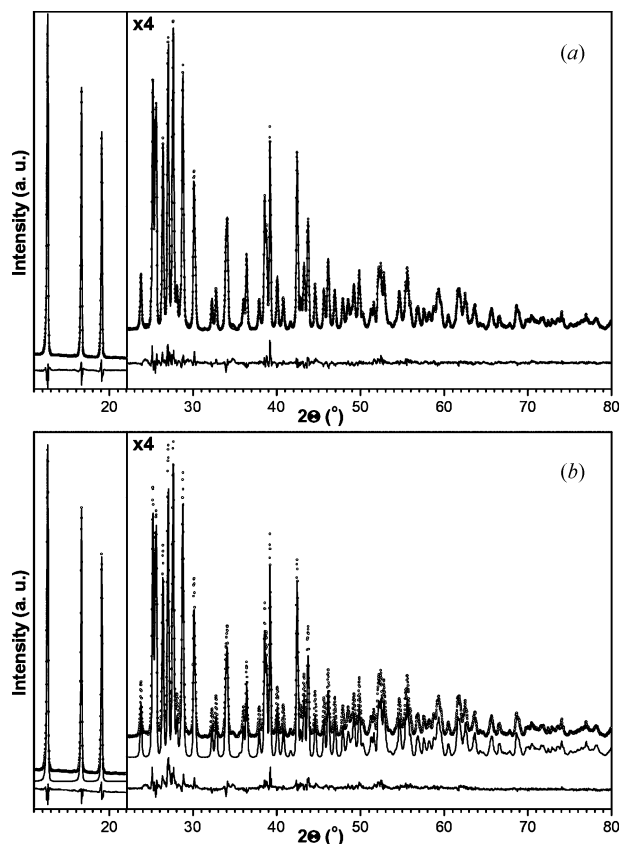

Figure 3
The experimental (circles), calculated (solid line) and difference (bottom curve) powder diffraction profiles after (*a*) Rietveld and (*b*) DDM refinement of the $[Pd(NH_3)_4](C_2O_4)$ structure.
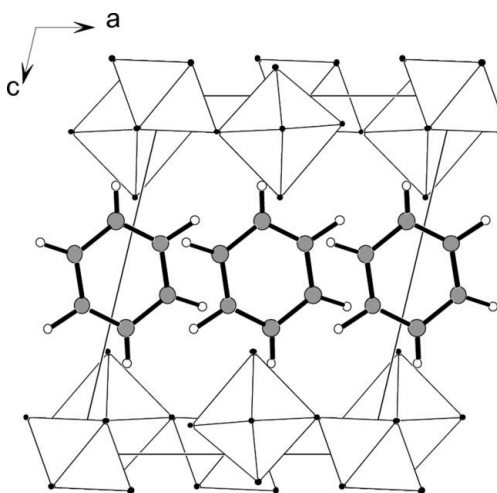

Figure 2
The $[Pd(NH_3)_4](C_2O_4)$ structure.

Figure 4
The $(C_5H_6N)Al_3F_{10}$ structure.

Table 5
Fractional atomic coordinates and isotropic displacement parameters (Å^2) for $(C_5H_6N)Al_3F_{10}$ obtained by DDM†.

	Occupancy	x	y	z	B_{iso}
Al1	1	0	0	0	0.3 (1)
Al2	1	−0.086 (3)	1/2	0.089 (3)	0.5 (2)
F1	1	−0.074 (1)	0.2012 (7)	0.092 (1)	1.4 (1)
F2	1	0.209 (1)	0	0.112 (2)	1.4 (1)
F3	1	−0.010 (2)	1/2	0.282 (2)	1.5 (3)
F4	1	0.131 (2)	1/2	0.069 (2)	1.4 (1)
C1‡	1	−0.152 (2)	0	0.471 (2)	3.1 (2)
C2‡	1	−0.088 (2)	0	0.358 (2)	3.1 (2)
C3‡	1	−0.075 (2)	0	0.608 (2)	3.1 (2)
H1§	0.5	−0.269 (5)	0.078 (4)	0.459 (5)	7.8 (8)
H2§	0.5	−0.141 (5)	0.078 (4)	0.300 (3)	7.8 (8)
H3	1	−0.137 (5)	0	0.673 (3)	7.8 (8)

† Displacement parameters were constrained for chemically equivalent atoms. ‡ The N atom was included in the refinement with an occupancy of 0.167 and its parameters were constrained to match those of the C atoms. § Atoms H1 and H2 are randomly displaced from the mirror plane.

performed using the shifted Chebyshev background functions and applying constraints on interatomic distances without which the structure geometry was not satisfactory (Harlow *et al.*, 1999). With DDM, the structure was refined successfully without constraints on interatomic distances (and without background modelling, of course). The structure parameters obtained by DDM are listed in Tables 2, 5 and 6. The difference curve of the final DDM plot shown in Fig. 5 demonstrates the complexity of the background line. As seen, even with such low-quality diffraction data, DDM allowed a satisfactory structure refinement.

The possibility of full-profile refinement independently of the background curve allowed by DDM is especially vital for semi-crystalline substances, such as polymers, organized amphiphilic liquid crystals and block copolymers, mesostructured materials *etc.*, for which the amorphous phase contribution to the background line is essential. A particular problem with mesostructured materials is that they exhibit diffraction peaks at very low angles, where the background is especially complex and difficult to model (Fig. 6). In the first applications of the full-profile structure analysis of meso-
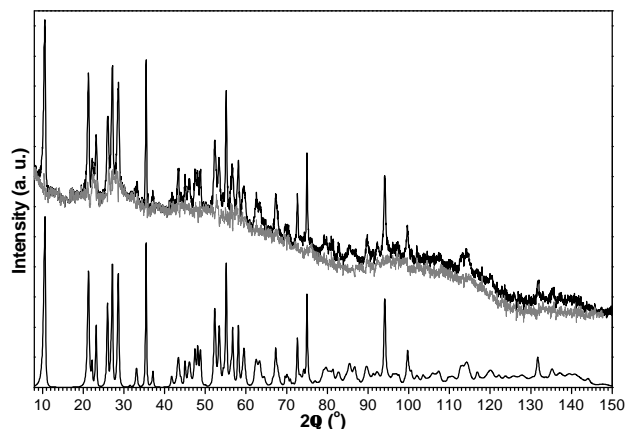
Table 6
Selected geometric parameters (Å, °) for $(C_5H_6N)Al_3F_{10}$.

Al1—F1[i]	1.772 (8)	F2—Al1—F1	92.5 (3)
Al1—F2	1.852 (13)	F2—Al1—F1[vi]	87.6 (3)
Al2—F3	1.979 (36)	F1[i]—Al1—F1	89.5 (3)
Al2—F2[ii]	1.767 (29)	F1[i]—Al1—F1[vi]	90.58 (3)
Al2—F4[iii]	1.615 (37)	F1[iii]—Al1—F3	86.1 (2)
Al2—F1[iv]	1.856 (5)	F3—Al2—F1	88.8 (3)
Al2—F4	1.855 (32)	F3—Al2—F2[ii]	87.0 (14)
C3—C2[v]	1.312 (23)	F3—Al2—F4	91.7 (15)
C2—C1	1.408 (31)	F2[ii]—Al2—F1	92.7 (3)
C1—C3	1.433 (28)	F4[iii]—Al2—F1	90.9 (3)
C2—H2[i]	0.821 (32)	F4[iii]—Al2—F4	83.2 (15)
C1—H1	1.063 (41)	C3[v]—C2—C1	109.5 (16)
C3—H3	0.944 (45)	C2—C1—C3	132.9 (19)
		C1—C3—C2[v]	117.6 (18)

Symmetry codes: (i) $x, -y, z$; (ii) $-\frac{1}{2}+x, \frac{1}{2}+y, z$; (iii) $-x, y, -z$; (iv) $x, 1-y, z$; (v) $-x, y, 1-z$; (vi) $-x, -y, -z$.

porous mesostructured materials using the continuous density function method (Solovyov, Kirik *et al.*, 2001*a,b*; Solovyov, Fenelonov *et al.*, 2001; Solovyov, Zaikovskii *et al.*, 2002; Solovyov, Shmakov *et al.*, 2002; Solovyov *et al.*, 2003), the background line was subtracted from the powder profile by the enhanced algorithm of Sonneveld & Visser (1975). This approximation was rough, but a trial background modelling with polynomials and other functions was absolutely unsatisfactory because of its very sharp change and complexity in the low-angle region. The use of DDM allows the solution of this problem. A first preliminary variant of DDM was applied in
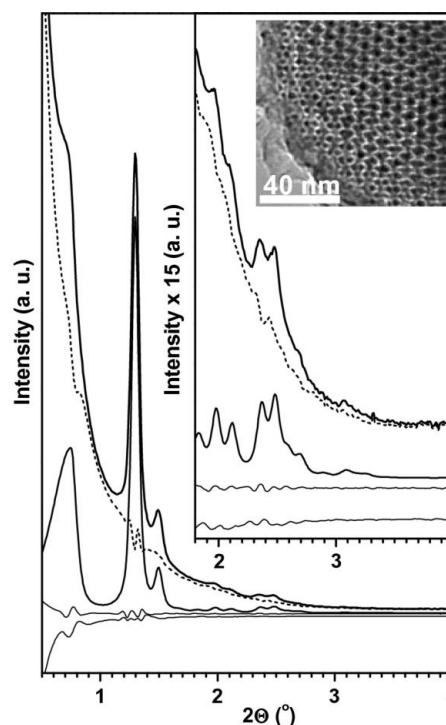

Figure 5
The experimental (top), calculated (bottom) and difference (middle grey) neutron powder diffraction profiles after the DDM refinement of the $(C_5H_6N)Al_3F_{10}$ structure.

Figure 6
The experimental (top), calculated (middle solid) and difference (middle dashed) small-angle synchrotron X-ray diffraction profiles of CMK-1 mesostructured carbon material after DDM structure refinement. The two bottom curves are the first and second derivatives of the difference profile. The insert shows a fragment of TEM image.

the full-profile X-ray diffraction structure analysis of a series of new silica mesoporous mesostructured materials (Kleitz *et al.*, 2003) and ordered nanopipe mesostructured carbons (Solovyov, Kim *et al.*, 2004). DDM allowed stable background-independent full-profile refinement of the structure parameters of these advanced nanomaterials, a result that was unattainable by any other method. To date, DDM has been applied to full-profile X-ray diffraction analysis of many different mesostructures, including a series of ordered silica mesoporous materials with either a three-dimensional cubic or a two-dimensional hexagonal lattice (Kleitz *et al.*, 2004) and mesostructured nanoframework carbons (Solovyov, Parmentier *et al.*, 2004).

In Fig. 6, a small-angle synchrotron X-ray diffraction profile of a mesostructured nanoframework carbon CMK-1 (Ryoo *et al.*, 1999; Parmentier *et al.*, 2002; Solovyov, Parmentier *et al.*, 2004) is compared with the calculated profile after DDM structure refinement. The material presents an ordered three-dimensional array of interwoven gyroidal carbon nanoframeworks formed within the pores of the silica MCM-48 (Monnier *et al.*, 1993) mesoporous template. The nanoframeworks are displaced with respect to one another after the silica wall dissolution, with a lowering of the initial material symmetry ($Ia3d$) inherited from the MCM-48 template, as shown by transmission electron microscopy (TEM) and X-ray diffraction (Kaneda *et al.*, 2002; Solovyov, Zaikovskii *et al.*, 2002). The DDM structure refinement performed utilizing the model density function developed for gyroidal mesostructures (Solovyov, Zaikovskii *et al.*, 2002) allowed the determination of the nanoframework thickness and displacement parameters for a series of CMK-1 carbons prepared using the chemical vapour deposition (Parmentier *et al.*, 2002) and liquid-phase infiltration methods (Ryoo *et al.*, 1999). Comprehensive comparative X-ray and TEM analysis of these materials revealed important correlations between the structure parameters and the synthesis procedures applied.

Besides the studies described above, the DDM procedure has also been tested on many other data sets and has demonstrated stable and correct full-profile refinement. Potential applications of DDM are not restricted to powder diffraction structure refinement only. Background-independent profile treatment can be especially desirable in quantitative phase analysis when amorphous admixtures must be accounted for. Future extensions of DDM may involve Bayesian probability theory, which has been utilized efficiently in background estimation procedures (von der Linden *et al.*, 1999; Fischer *et al.*, 2000; David & Sivia, 2001) and Rietveld refinement in the presence of impurities (David, 2001). DDM will also be useful at the initial steps of powder diffraction structure determination when the structure model is absent and the background line cannot be defined correctly. The direct space search methods of structure solution, such as simulated annealing (Solovyov & Kirik, 1993) and others, may efficiently utilize background-independent DDM. Moreover, DDM can be applicable in many other data treatment procedures where sharp peaks and slowly oscillating background need to be separated.

4. Conclusions

The derivative difference minimization method of full-profile refinement developed in this work is shown to be a very powerful and efficient tool of powder diffraction structure analysis. The most attractive advantage of DDM is the possibility of profile refinement without background line modelling. Moreover, when properly applied, this method may allow the derivation of structure parameters with even higher quality than can be obtained by Rietveld refinement in the presence of systematic errors in the model background function. The principles of DDM are universal and may be used in many different areas of powder diffraction and beyond. Future developments will be focused on studying the properties of this procedure and its efficiency in applications to data of a different nature. Different options for calculating the derivative difference minimization function and various refinement strategies should be subjected to methodical analysis.

References

David, W. I. F. (2001). *J. Appl. Cryst.* **34**, 691–698.
David, W. I. F. & Sivia, D. S. (2001). *J. Appl. Cryst.* **34**, 318–324.
Fischer, R., Hanson, K. M., Dose, V. & von der Linden, W. (2000). *Phys. Rev. E*, **61**, 1152–1160.
Harlow, R. L., Herron, N., Li, Z., Vogt, T., Solovyov L. & Kirik, S. (1999). *Chem. Mater.* **11**, 2562–2567.
Kaneda, M., Tsubakiyama, T., Carlsson, A., Sakamoto, Y., Ohsuna, T., Terasaki, O., Joo S. H. & Ryoo, R. (2002). *J. Phys. Chem. B*, **106**, 1256–1266.
Kleitz, F., Liu, D., Anilkumar, G. M., Park, I.-S., Solovyov, L. A., Shmakov, A. N. & Ryoo, R. (2003). *J. Phys. Chem. B*, **107**, 14296–14300.
Kleitz, F., Solovyov, L. A., Anilkumar, G. M., Choi, S. H. & Ryoo, R. (2004). *Chem. Commun.* pp. 1536–1537.
McCusker, L. B., Von Dreele, R. B., Cox, D. E., Louer, D. & Scardi, P. (1999). *J. Appl. Cryst.* **32**, 36–50.
Monnier, A., Schuth, F., Huo, Q., Kumar, D., Margolese, D., Maxwell, R. S., Stucky, G. D., Krishnamurty, M., Petroff, P., Firouzi, A., Janicke, M. & Chmelka, B. F. (1993). *Science*, **261**, 1299–1303.
Parmentier, J., Patarin, J., Dentzer, J. & Vix-Guterl, C. (2002). *Ceram. Int.* **28**, 1–7.
Riello, P., Fagherazzi, G., Clemente, D. & Canton, P. (1995). *J. Appl. Cryst.* **28**, 115–120.
Rietveld, H. (1969). *J. Appl. Cryst.* **2**, 65–71.
Ryoo, R., Joo, S. H. & Jun, S. (1999). *J. Phys. Chem. B*, **103**, 7743–7746.
Savitzky, A. & Golay, M. J. E. (1964). *Anal. Chem.* **36**, 1627–1639.
Solovyov, L. A., Belousov, O. V., Shmakov, A. N., Zaikovskii, V. I., Joo, S. H., Ryoo, R., Haddad, E., Gedeon, A. & Kirik, S. D. (2003). *Stud. Surf. Sci. Catal.* **146**, 299–302.
Solovyov, L. A., Blochina, M. L., Kirik, S. D., Blokhin, A. I. & Derikova, M. G. (1996). *Powder Diffr.* **11**, 13–16.
Solovyov, L. A., Blokhin, A. I., Mulagaleev, R. F. & Kirik, S. D. (1999). *Acta Cryst.* C**55**, 293–296.
Solovyov, L. A., Fenelonov, V. B., Derevyankin, A. Y., Shmakov, A. N., Haddad, E., Gedeon, A., Kirik, S. D. & Romannikov, V. N. (2001). *Stud. Surf. Sci. Catal.* **135**, 287.
Solovyov, L. A., Kim, T.-W., Kleitz, F., Terasaki, O. & Ryoo, R. (2004). *Chem. Mater.* **16**, 2274–2281.

Solovyov, L. A. & Kirik, S. D. (1993). *Mater. Sci. Forum*, **133–136**, 195–200.

Solovyov, L. A., Kirik, S. D., Shmakov, A. N. & Romannikov, V. N. (2001*a*). *Microporous Mesoporous Mater.* **44**, 17–23.

Solovyov, L. A., Kirik, S. D., Shmakov, A. N. & Romannikov, V. N. (2001*b*). *Adv. X-ray Anal.* **44**, 110–115.

Solovyov, L. A., Parmentier, J., Ehrburger-Dolle, F., Werckmann, J., Vix-Guterl, C. & Patarin, J. (2004). *Fourth International Mesostructured Materials Symposium, Abstracts*, May 1–4, 2004, pp. 358–359.

Solovyov, L. A., Shmakov, A. N., Zaikovskii, V. I., Joo, S. H. & Ryoo, R. (2002). *Carbon*, **40**, 2477–2481.

Solovyov, L. A., Zaikovskii, V. I., Shmakov, A. N., Belousov, O. V. & Ryoo, R. (2002). *J. Phys. Chem. B*, **106**, 12198–12202.

Sonneveld, E. J. & Visser, J. V. (1975). *J. Appl. Cryst.* **8**, 1–7.

Linden, W. von der, Dose, V., Padayachee, J. & Prozesky, V. (1999). *Phys. Rev. E*, **59**, 6527–6534.

Wiles, D. B. & Young, R. A. (1981). *J. Appl. Cryst.* **14**, 149–151.

Young, R. A. (1993). Editor. *The Rietveld Method*. Oxford University Press.

Leonid A. Solovyov · Derivative difference minimization **749**